

PID-based P&O MPPT Controller for Offgrid Solar PV Systems Using Ziegler-Nichols Tuning Method to Step, Ramp and Impulse Inputs

Emmanuel Kwaku Anto

Dept. of Electrical & Electronics Engineering
KNUST
Kumasi, Ghana
kwakuantoh@yahoo.com;
ekanto.soe@knust.edu.gh

Johnson A. Asumadu

Western Michigan University
Kalamazoo, MI, 49008
USA

johnson.asumadu@wmich.edu

Philip Yaw Okyere

Dept. of Electrical & Electronics Engineering
KNUST
Kumasi, Ghana
okyerepy@yahoo.com

Abstract— In this paper, PID-based MPPT controller is designed for offgrid solar photovoltaic (PV) system. The Ziegler-Nichols (Z-N) Reaction Curve Tuning Method is employed to obtain the tuned response, and from that the tuned performance parameters as well as the optimum PID gain parameters. The responses of the system to step, ramp and impulse inputs are then compared with those of the offgrid solar photovoltaic (PV) system WITH and WITHOUT the Perturb-and-Observe (P&O) Maximum Power Point Tracking (MPPT).

The study shows the superiority the PID-controlled MPPT system over the P&O MPPT and the non-MPPT systems for all the various signal inputs. In particular, the simulated response of the PID-based system to the step input gave the shortest settling time of 22.7 ms (indicating the fastest system response) and zero overshoot (representing minimum losses). The system with P&O MPPT performance placed second with a settling time of 30 ms and 224 % overshoot. The non-MPPT system gave the slowest response with a settling time of 38.5 ms.

Keywords—PV system; Maximum Power Point Tracking (MPPT); Ziegler-Nichols (Z-N) tuning; Proportional-Integral-Derivative (PID); Perturb-and Observe (P&O); Photovoltaic (PV)

I. INTRODUCTION

The world is witnessing energy crisis and rising environment pollution. In order to solve these problems, emphasis is being placed on clean, non-polluting renewable sources of energy. Photovoltaic energy is of great importance in this regard as it is clean, inexhaustible and widely available.

The use of PV technology has several challenges. One such challenge is that it does not provide a constant energy source because its output power changes with temperature and insolation level. Thus it becomes difficult to extract the maximum available power from pv modules [1]. To overcome this challenge a Maximum Power Point Tracker (MPPT) is used.

Most of the existing conventional MPPT algorithms (like the P&O control algorithm) are unable to achieve optimum power tracking and even when they do, take a long time to do so. This has therefore necessitated the use of an improved or hybridized MPPT control algorithm to achieve better PV output performance. The PID-controlled MPPT algorithm is one such improved control algorithm. The biggest problem of using the PID controller is tuning its parameters to achieve optimum performance [4]. Many techniques have been proposed in the literature to achieve the best tuning [5-8].

Very good performance parameters such as overshoot, settling time, rise time and steady-state offset have been recorded with hybrid artificial-intelligence (AI) based systems. However, their implementation has not been very easy because of the complexity of the processes and the high computations involved. There is therefore the need for a trade-off or compromise between accuracy of results and simplicity of the computational process.

In this paper, a suitable compromise has been proposed using the PID control strategy. For the tuning of the PID, the Ziegler-Nichols Tuning Method with the Reaction Curve was employed. The proposed method offers a number of merits. Firstly, the Z-N tuning method is a tried and tested approach that has stood the test of time. Secondly, it is a much simpler approach compared to the existing AI-based algorithms which involved more complex tracking processes. Thirdly, even though the PID is a linear system, it can be used to control non-linear systems [4].

The PID-based P&O MPPT controlled offgrid solar PV system was modeled and simulated in MATLAB/SIMULINK. The results showed very good output performance with PID controller for the various step, ramp and impulse inputs.

II. THE OFFGRID SOLAR PV SYSTEM MODEL

A standalone solar PV system basically consists of the PV array, DC-DC converter and an MPPT control system. Fig. 1 shows a block diagram of a standalone PV system with PV modules, MPPT, DC-DC converter and controller and connected load [9].

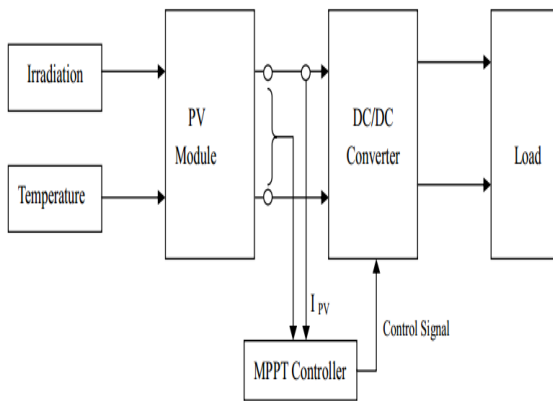


Fig. 1. Block Diagram of PV System with PV Module, MPPT Controller, DC-DC Converter [9]

The output current and voltage of the PV module are used as input parameters for the MPPT controller, which issues the appropriate command signal to the DC-DC converter which acts as interface between the load and module.

A. Model of PV Module

A PV module consists of many PV cells connected in parallel to increase the PV current and in series to provide high output voltage. The equivalent circuit of a practical PV module is shown in Fig 2 [14, 26], The DC current I_{PV} , generated by the module depends on solar irradiance, temperature, and load current.

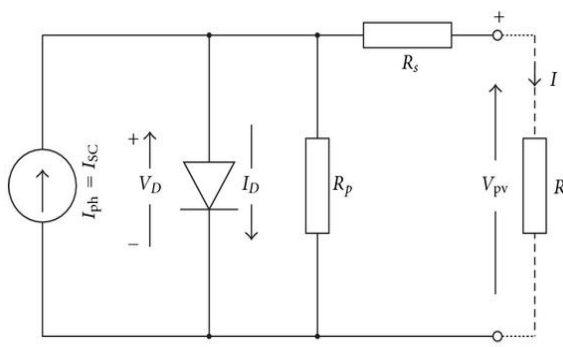


Fig. 2. Practical Equivalent PV Cell Model having a single diode with series and parallel resistances [14, 26]

The shunt resistance R_p accounts for the losses due to the leakage currents across the p-n junction and within the cell due to crystal imperfections and impurities, whilst the series resistance R_s represents the losses due to the module's internal series resistance, contacts and cell interconnections [14].

The fundamental equations that describe the current-voltage (I-V) characteristic of the PV cell are as follows:

$$V_D = V + IR_s \quad (1)$$

$$I_D = I_0 \left[\exp\left(\frac{V_D}{a \times V_t}\right) - 1 \right] \quad (2)$$

$$I = I_{Ph} - I_D - \frac{V_D}{R_p} \quad (3)$$

or

$$I = I_{Ph} - I_0 \left[\exp\left(\frac{V_{pv} + IR_s}{a \times V_t}\right) - 1 \right] - \frac{V_{pv} + IR_s}{R_p} \quad (4)$$

Where

I_0 is the diode reverse saturation current

I_{Ph} is the photocurrent,

V_D is the voltage across the diode,

a is the diode ideality factor which depends on the PV technology [14].

$$V_t = \frac{kT}{q} \text{ is the thermal voltage} \quad (5)$$

k is Boltzmann's constant ($1.3806503 \times 10^{-23}$ J/K),

T is the temperature of the p-n junction in degrees Kelvin, and

q is electron charge ($1.6021764 \times 10^{-19}$ C).

For a module composed of N_p parallel connections of cells, and N_s number of PV cells connected in series, the photovoltaic and saturation currents may be expressed as [10]:

$$I_{Ph}(\text{module}) = I_{Ph} \times N_p; \quad (6)$$

$$I_0(\text{module}) = I_0 \times N_p \quad (7)$$

The output current of the PV module is given as [10]:

$$I = N_p I_{ph} - N_p I_0 \left[\exp \left(q \times \frac{(V_{pv} + IR_s)}{N_s akT} \right) - 1 \right] - \frac{V_{pv} + IR_s}{R_p} \quad (8)$$

With the current technology in the manufacture of the PV cell, the leakage current across the p-n junction is negligible, that is $R_p \cong \infty$. Since the shunt resistance is very large compared to the series resistance R_s , it can be represented as an open-circuit [15]. Hence the I-V characteristic equation of a PV module reduces to

$$I = N_p I_{ph} - N_p I_0 \left[\exp \left(q \times \frac{(V_{pv} + IR_s)}{N_s akT} \right) - 1 \right] \quad (9)$$

The SIMULINK model of the current of Eqn. (9) is shown in Fig. 3.

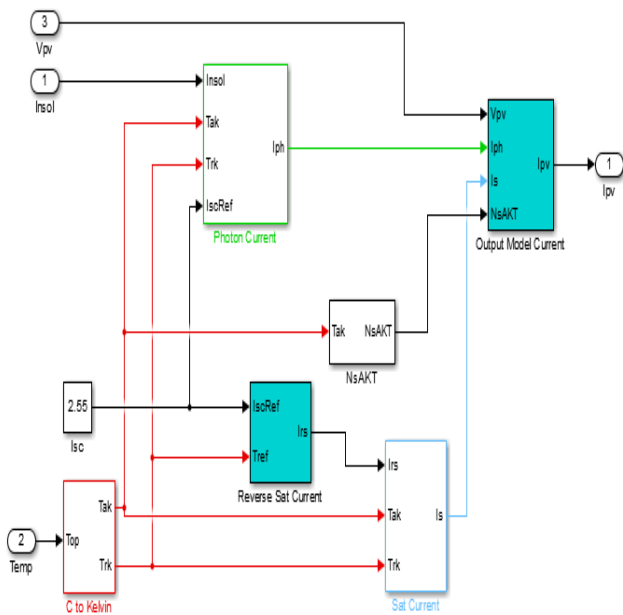


Fig. 3. SIMULINK Model of PV output current

B. DC-DC Converter Model

The three main types of DC-DC converters used are the Buck Converter, the Boost Converter and Buck Boost Converter [17]. In this paper, the DC-DC boost converter is used. The mathematical equations for the boost converter are as follows:

$$V_{out} = \frac{1}{1-D} V_{in} \quad (10)$$

$$D = \frac{t_{on}}{t_{on} + t_{off}} \quad (11)$$

$$t_{on} = D \times T_s \quad (12)$$

$$t_{off} = (1-D)T_s \quad (13)$$

$$T_s = 1/f_s \quad (14)$$

D is the duty cycle of the converter, t_{on} and t_{off} are the on-off times respectively, T_s is the switching period and f_s is the system frequency.

The output voltage is changed by varying the duty cycle.

The SIMULINK model of the DC-DC converter is shown in Fig.4.

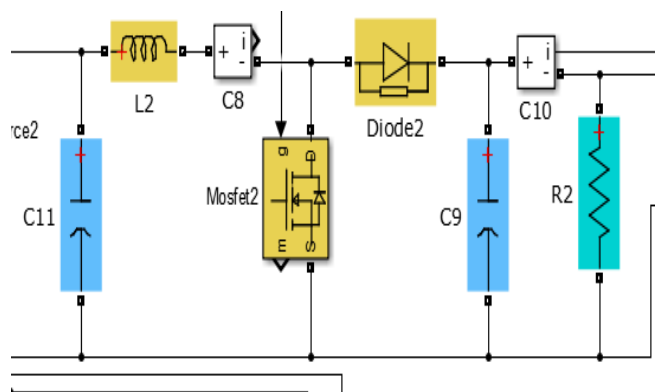


Fig. 4. SIMULINK Model of the DC-DC converter

The parameters L and C were determined using the design equations (15) and (16) [18]

$$L_{min} = \frac{(1-D)^2 \times D \times R}{2f_s} \quad (15)$$

$$C_{min} = \frac{DV_{out}}{R \times f_s \times V_r} \quad (16)$$

$$V_r = \frac{\Delta V_{out}}{V_{out}} \quad (17)$$

L_{min} is the minimum inductance, D is the duty cycle, R is the output resistance, f_s is the switching frequency, C_{min} is minimum capacitance and V_r is the output ripple voltage.

C. The P&O Algorithm

The P&O is the most commonly used MPPT algorithms to track the maximum power point of the PV system, due to its ease and low-cost of implementation.

The P&O algorithm finds the maximum power point (MPP) of PV modules by iteratively perturbing the array voltage V , observing and comparing the power

generated by the PV modules $P(n)$ at any instant with the previous power $P(n-1)$. The voltage perturbation is achieved through the change in the duty cycle D .

The increment or decrement of the duty cycle D in every sampling period is determined by the comparison of the power at present time and previous time. If $dP = P(n) - P(n-1) > 0$, the duty cycle is increased and if $dP < 0$, the duty cycle is then reduced.

The duty cycle perturbation is stopped when $dP = 0$ or practically equal to a small preset value [21]. Fig 1 shows the flowchart of the P&O algorithm with duty cycle perturbation [13].

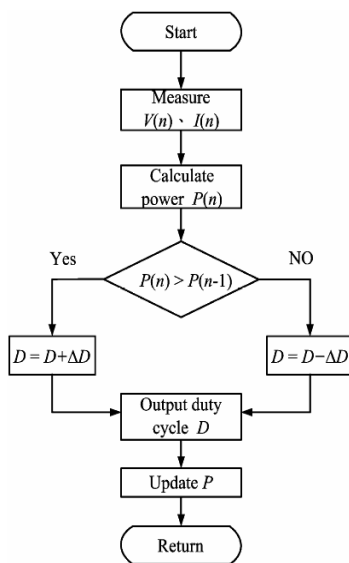


Fig. 5. Flowchart of the P&O Algorithm using duty cycle perturbation [13]

D. The P&O Perturbation Methods

Three main methods of P&O perturbation have been proposed and used. These are:

1. **Reference voltage perturbation** [22] – In this method, the PV array output reference is used as the control parameter in conjunction with a controller (usually a PID) to adjust the duty ratio of the MPPT power converter.
2. **Reference current perturbation** [23] - The reference current perturbation approach uses the PV array output current reference as the control parameter. Due to its slow transient response to irradiance changes and high susceptibility to noise and a proportional-integral (PI) controller oscillation, the reference current control is not widely used.
3. **Direct duty ratio perturbation** [24] - The direct duty ratio perturbation uses duty ratio of the MPPT converter directly as the control parameter

III. THE PID CONTROLLER

The proportional-integral-derivative (PID) controller is the most common control algorithm used in industry and has been universally accepted in industrial control. The popularity of PID controllers can be attributed partly to their robust performance in a wide range of operating conditions and partly to their functional simplicity, which allows engineers to operate them in a simple, straightforward manner [2].

The block diagram of the PID controller is shown in Fig.6.

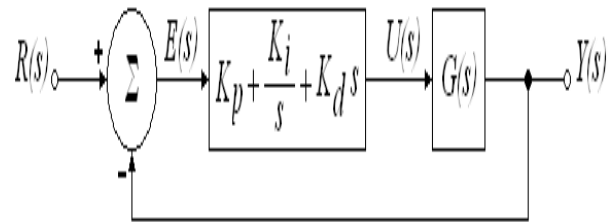


Fig. 6. Block Diagram of PID Controller

Although the PID controller is a linear controller, it can be used to control many nonlinear and industrial systems with a much better performance. However it has less robustness against uncertainty [4]

Many various tuning methods have been proposed from 1942 up to now for gaining better and more acceptable control system response based on desirable control objectives such as percent of overshoot, integral of absolute value of the error (IAE), settling time, manipulated variable behavior, etc. [3].

Some of the tuning methods have considered only one of the above objectives as a criterion for their tuning algorithm and some of them have developed their algorithm by considering more than one of the mentioned criteria.

The Ziegler-Nichols (Z-N) proportional, integral and derivative gain parameters K_p , K_i , and K_d respectively are found by generating an S-shaped step response for the system (see Fig 7) and using it to determine its time constant T and its delay time L .

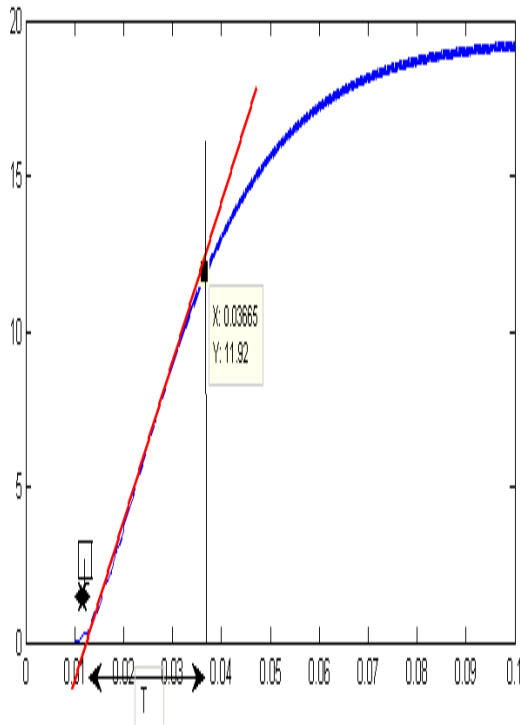


Fig. 7. Ziegler-Nichols (Z-N) Reaction Curve

The gain parameters are calculated using the above two parameters T and L as follows:

$$K_p = K_c \quad (18)$$

$$K_i = \frac{K_p}{T_i} \quad (19)$$

$$K_d = K_p \times T_d \quad (20)$$

where K_c is the critical gain, and is given by (21) as

$$K_c = \frac{T}{L} \quad (21)$$

T_i is the integral time, and is given by (22) as

$$T_i = 2L \quad (22)$$

T_d is the derivative time, and is given by (23) as

$$T_d = 0.5L \quad (23)$$

From the curve of Fig 7, the parameters $L = 0.01305$ s, and $T = 0.02665$ s. Substituting these values into (21), (22) and (23), the critical gain, integral time and derivative time are obtained as $K_c = 2.0421$, $T_i = 0.0261$ and $T_d = 0.006525$, respectively.

Subsequently, the derived Z-N proportional, integral and derivative gain parameters for the PID controller are obtained from (18), (19) and (20) as $K_p = 2.4505$, $K_i = 93.8927$ and $K_d = 0.0159$ respectively.

The Z-N derived PID gain/tuning parameters are applied to the modeled PID controller in SIMULINK to obtain the *tuned response*, and from that the tuned performance parameters as well as the *optimum PID gain parameters*

IV. THE SOLKAR 36W TEST MODULE PARAMETERS

The SOLKAR 36W PV module was selected as the test module for simulation. The manufacturer's data sheet details for the test module are given in Table I. In addition to that, the series resistance (R_s) of PV module is taken as 0.2Ω , the band gap energy (E_g) of the semiconductor used was taken as 1.1 eV, the diode ideality factor (a) of the semiconductor was taken as 1.6, electron charge q as $1.60217646 \times 10^{-19} \text{C}$, the temperature coefficient K_I as 0.0017 and Boltzmann constant k as $1.3806503 \times 10^{-23} \text{J/K}$.

TABLE I. SOLKAR 36W MODULE PARAMETERS

| Model Characteristic | Parameter | Value | Unit |
|--------------------------------------|-----------|-------|------|
| Open-circuit voltage | V_{oc} | 21.24 | V |
| Maximum voltage | V_{mp} | 16.56 | V |
| Short-circuit current | I_{sc} | 2.55 | A |
| Current at maximum power | I_{mp} | 2.25 | A |
| Rated power | P | 37.26 | W |
| Number of series cells | N_s | 36 | |
| Number of parallel connected modules | | 4 | |
| Number of series connected modules | | 2 | |

V. METHODOLOGY

The PV system was modeled in MATLAB/SIMULINK environment using the SIMSCAPE and SIMULINK libraries. The SOLKAR 36W PV module was simulated using the parameters given in Table I. The DC-DC boost converter was simulated using the SIMSCAPE library. The MPPT algorithm implemented was the P&O, and was simulated using a MATLAB function in MATLAB/SIMULINK.

Three offgrid solar PV systems were modeled:

- (i) system WITHOUT MPPT,
- (ii) P&O MPPT system (open-loop), and
- (iii) PID-controlled MPPT system (closed-loop).

The irradiance of the system was then varied from zero to the standard value of 1000 W/m² for step, ramp and impulse variations, while keeping the temperature constant at 25°C (298°K) for the systems. The output powers of the three systems were then obtained using a display and a scope.

For the determination of the *closed-loop* performance parameters, the Ziegler-Nichols Reaction Curve Tuning Method was employed to derive the initial, non-optimum Z-N tuning parameters. The Z-N tuning parameters so derived were applied to the PID controller modeled in MATLAB/SIMULINK, and simulated with the various step, ramp and impulse inputs to obtain the tuned/optimum responses with the PID controller.

The *optimum performance parameters* of the various tuned responses were obtained, together with the corresponding optimum gain parameters K_p , K_i , and K_d , and then compared.

VI. PV ARRAY SIMULINK MODELING

The PV array was modelled using the current equation (25) of the PV panel. The parameters used for the model are as given in Table I.

$$I = N_p I_{Ph} - N_p I_0 \left[\exp \left(q \times \frac{(V_{pv} + IR_s)}{N_s akT} \right) - 1 \right] \quad (24)$$

The equation (24) was modeled in 6 parts:

- Temperature conversion model
- Model of photocurrent I_{Ph}
- Model of reverse saturation current I_{rs}
- Model of the diode saturation current I_0
- Model of operating $N_s akT$
- Model of the PV current equation I

A. Temperature conversion model

This model is used for the conversion of the module operating and reference temperatures from degree Celsius to Kelvin.

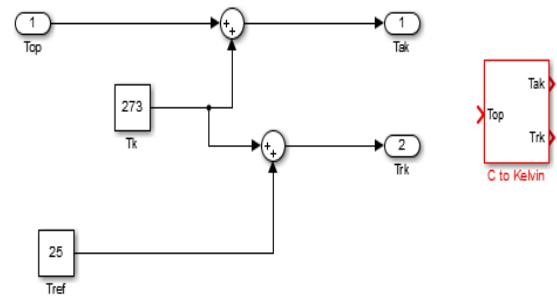


Fig. 8. Temperature conversion model in SIMULINK

B. Model of photocurrent I_{Ph}

The SIMULINK model shown in Fig. 9 is used to implement the photocurrent equation (25).

$$I_{Ph} = G * [I_{sc} + K_I (T - T_r)] \quad (25)$$

I_{sc} is the cell short-circuit current at a 25 °C and 1kW/m², K_I is the cell short-circuit current temperature coefficient, T_r is the cell reference temperature, and G is the solar insolation in kW/m².

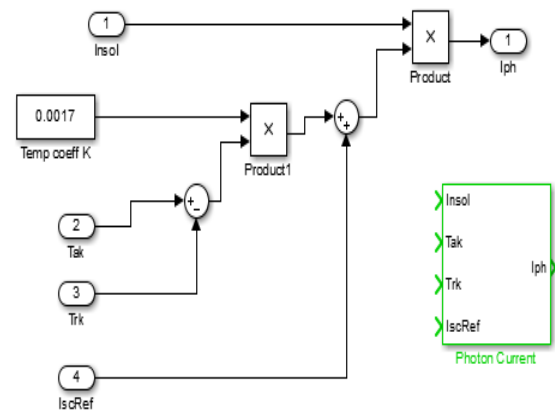


Fig. 9. Photocurrent model in SIMULINK

C. Model of reverse saturation current I_{rs}

The reverse saturation current was modelled based on equation (26) using commonly used blocks in SIMULINK library. It takes in the short-circuit current at the reference temperature and the module reference temperature as inputs.

$$I_{rs} = \frac{I_{sc}}{\exp \left[\frac{qV_{oc}}{N_s akT} \right] - 1} \quad (26)$$

The SIMULINK model for the reverse saturation current using equation (26) is shown in Fig 10.

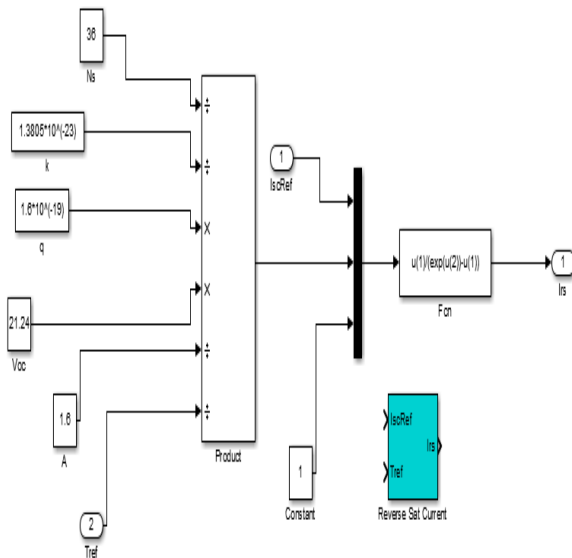


Fig. 10. Reverse saturation current model in SIMULINK

D. Model of diode saturation current I_0

The saturation current was modelled based on the equation (27) using the commonly used block in the SIMULINK library. The model takes the reverse saturation current, module reference temperature and the module operating temperature as inputs and calculates the module diode saturation current.

$$I_0 = I_{rs} \left[\frac{T}{T_r} \right]^3 \exp \left[q * E_g \left(\frac{1}{T_r} - \frac{1}{T} \right) \right] \quad (27)$$

The SIMULINK model for the diode saturation current using equation (27) is shown in Fig 11.

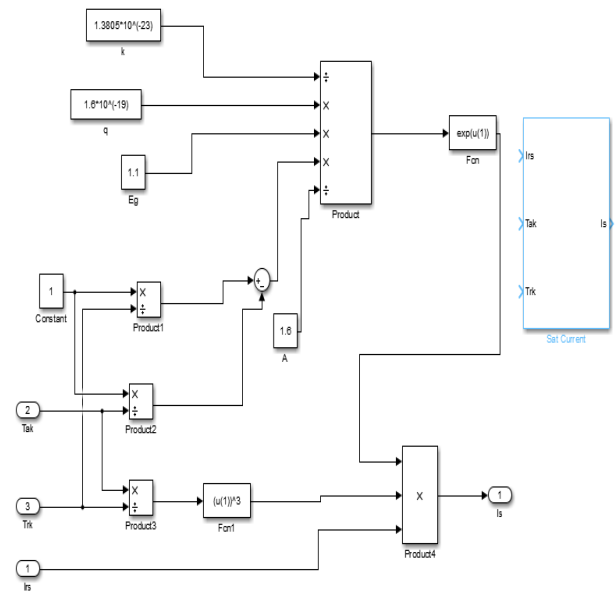


Fig. 11. Diode saturation current model in SIMULINK

E. Model of $N_s akT$ product

This was modeled using elements from the commonly used block in SIMULINK library. It takes the module operating temperature in Kelvin and calculates the $N_s akT$. The model of the product $N_s akT$ is used in the PV current equation model shown in Fig. 12.

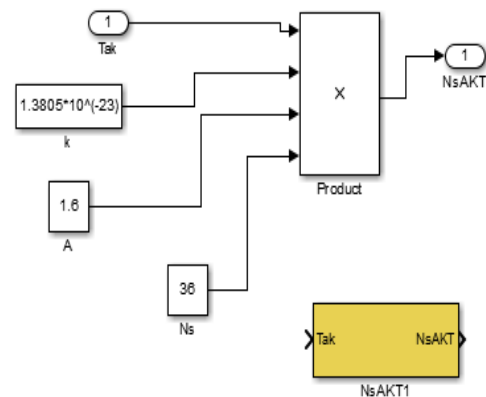


Fig. 12. Model of $N_s kaT$ product in SIMULINK

F. Model of PV current equation I

The output current of the PV module is based on equation (28). It is modelled using the commonly used block library. The inputs were connected to a multiplexer, which is then connected to a user defined function to obtain the current I . The equation used in this function (fcn) is

$$I = u(3) - u(4) * [\exp((u(2) \cdot u(1) + u(6)) / (u(5))) - 1] \quad (28)$$

Where $u(a)$ represents the inputs on the multiplexer and the “a” represents the position of the input on the multiplexer. The SIMULINK model for the PV current using equation (28) is as already shown in Fig 3.

G. Interconnected subsystems of PV module in SIMULINK

Fig. 13 shows the interconnection of all the six Simulink models masked and interconnected together to get the PV array. The model takes irradiance, operating temperature and voltage as inputs to produce the PV current.

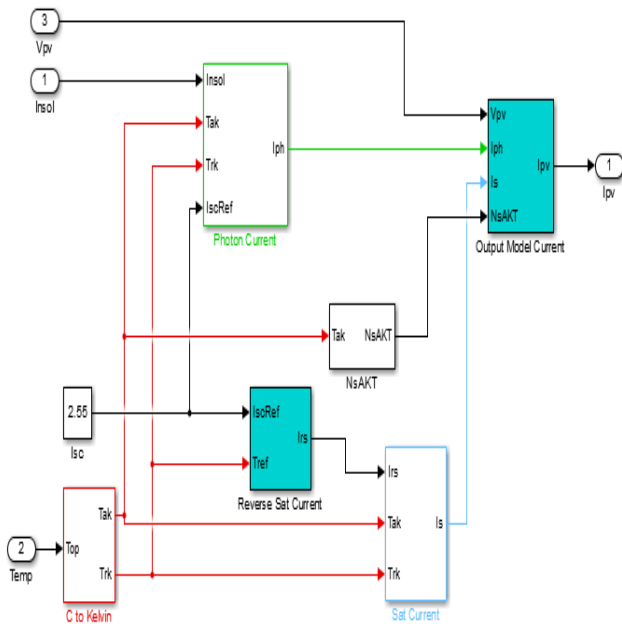


Fig. 13. Interconnected subsystems of PV current in SIMULINK

VII. DC-DC BOOST CONVERTER MODELING

The boost converter was simulated using electronic elements from SIMSCAPE in the SIMULINK library. Based on equations (15) and (16), the capacitance and inductance were calculated to obtain the parameters in Table II. A DC voltage of 12V is fed into the converter in place of the PV module.

TABLE II. BOOST CONVERTER PARAMETERS

| Model Characteristic | Parameter |
|-----------------------|-------------|
| Inductance, L | 290 μ H |
| Capacitor, C (output) | 470 μ F |
| Capacitor, C (input) | 330 μ F |
| DC voltage | 12 V |
| Load, R | 50 Ω |
| Switching frequency | 5000 Hz |

The SIMULINK model for the DC-DC boost converter is as already shown in Fig 4.

VIII. MPPT CONTROLLER MODELING

The MPPT was simulated using a MATLAB function from the SIMULINK library to produce the codes based on the P&O algorithm. The MPPT is connected to the converter which takes its voltage from the PV panel. The duty cycle is fed into the converter through the PWM generator. The P&O algorithm was simulated according to the flowchart of Fig. 3, and the SIMULINK model is shown in Fig. 14.

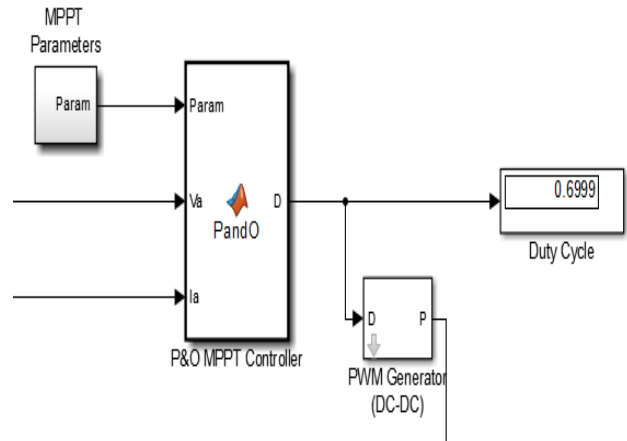


Fig. 14. MPPT Controller SIMULINK Model

IX. PID CONTROLLER MODELING

The PID controller was employed to simulate the closed loop PV characteristics. To obtain the optimum gain parameters, the Ziegler-Nichols tuning method was employed, as described in Section III. The full PID control mode was used since it encompasses all aspects and parameters of PID control.

X. COMPLETE MODEL OF THE PID-BASED SOLAR PV SYSTEM WITH P&O MPPT

Fig. 15 shows the complete simulation of the PV system consisting of the PV module, the boost converter, the MPPT and the load. The inputs are temperature and insolation. The results are displayed using displays and scopes.

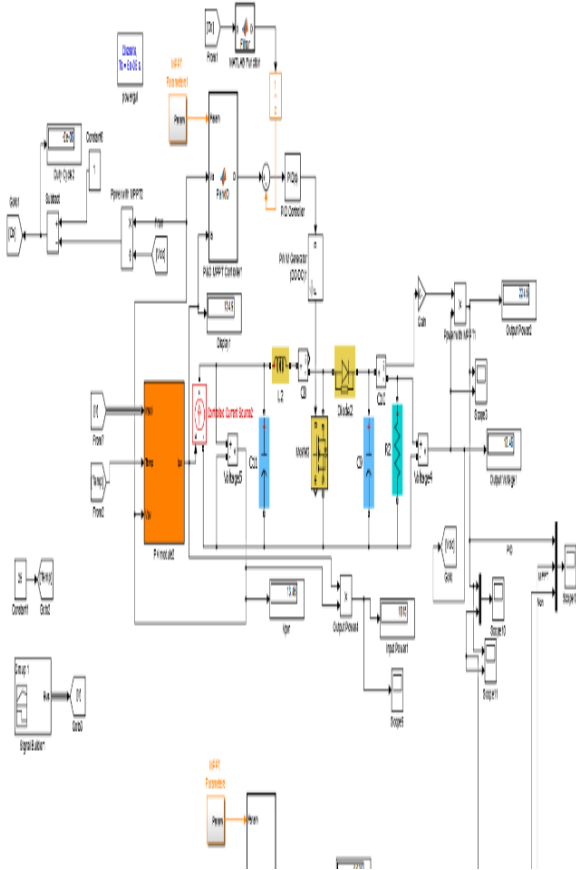


Fig. 15. Complete SIMULINK Model of PID-based Solar PV System with P&O MPPT

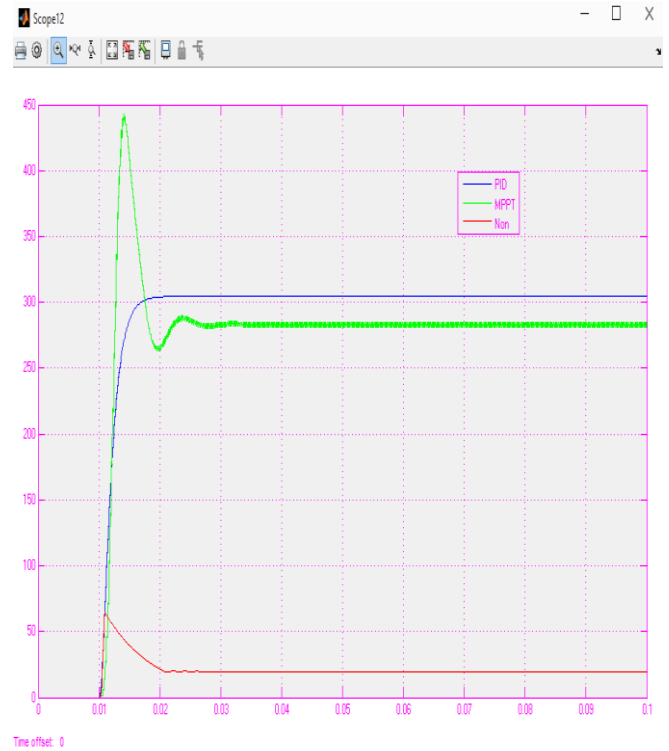


Fig. 16. STEP Response for NO MPPT, P&O MPPT (open-loop) and PID-based MPPT (closed-loop)

The resulting response parameters are as tabulated in Table III.

TABLE III. PERFORMANCE PARAMETERS FOR STEP INPUT

| Performance Parameter | NO MPPT | P&O MPPT (open-loop) | PID-based MPPT (closed-loop) |
|-----------------------|---------|----------------------|------------------------------|
| Overshoot (%) | 55.9 | 224 | 0 |
| Settling time (ms) | 38.5 | 30 | 22.7 |
| Rise time (ms) | 13.4 | 10.9 | 14.2 |

XI. SIMULATION RESULTS AND ANALYSES

In this section, the responses of the P&O MPPT (open-loop) and PID-based control (closed-loop) solar PV system to step, ramp and impulse inputs are presented and analyzed.

For a 1000 W/m² irradiance, the maximum power for the 2-by-4 array is calculated with equation (29) as

$$\begin{aligned}
 P_{MPP} &= V_{MP} \times I_{MP} \times \text{Number parallel connected} \\
 &\quad \text{modules} \times \text{Number series connected modules} \\
 &= 16.56 \times 2.25 \times 4 \times 2 \\
 &= 298.08 \cong 300 \text{ W}
 \end{aligned}
 \tag{29}$$

A. Step Response

Analyses of open-loop and closed-loop step responses are presented in this section. Fig. 16 shows the PV output power in response to a **step irradiance input**.

The following **step response analyses** can be made from Fig 16 and Table III:

1. The maximum attainable PV output power is $P_{MPP} \cong 300 \text{ W}$ (23). But from Fig 16, the best realized PV output power for NO MPPT is about 56 W, far below the maximum attainable output power.

2. This virtual under-utilization of the PV output power is not good, and necessitates an improvement through the use of an MPPT.

3. The *P&O MPPT open-loop* parameters represent the base case scenario or reference performance.

4. By employing a P&O MPPT control, the maximum power was ultimately nearly obtained after a

settling time of about 0.04 s, albeit with expected ripples and oscillations around the MPP.

5. The high open-loop percentage overshoot of 224 % represents a huge increase in losses which need to be controlled or reduced.

6. The PID-based MPPT represents a closed-loop control, and offers the best performance. The maximum output power was not only attained, but was also achieved with theoretically no overshoot.

7. This zero overshoot signifies ideally no losses or practically a very huge reduction in losses.

8. Also, the settling time with PID-MPPT control was correspondingly reduced from an open-loop value of 30 ms with P&O MPPT to the closed-loop value of 22.7 ms with PID MPPT, which happens to be the minimum of the settling times.

9. This denotes an achievement of an overall fastest system response with PID MPPT control.

10. The rise time, however, witnessed an increase from 10.9 ms to 14.2 ms.

B. Ramp Response

Analyses of open-loop and closed-loop ramp responses are presented in this section. Fig. 17 shows the PV output power in response to a ramp irradiance input.

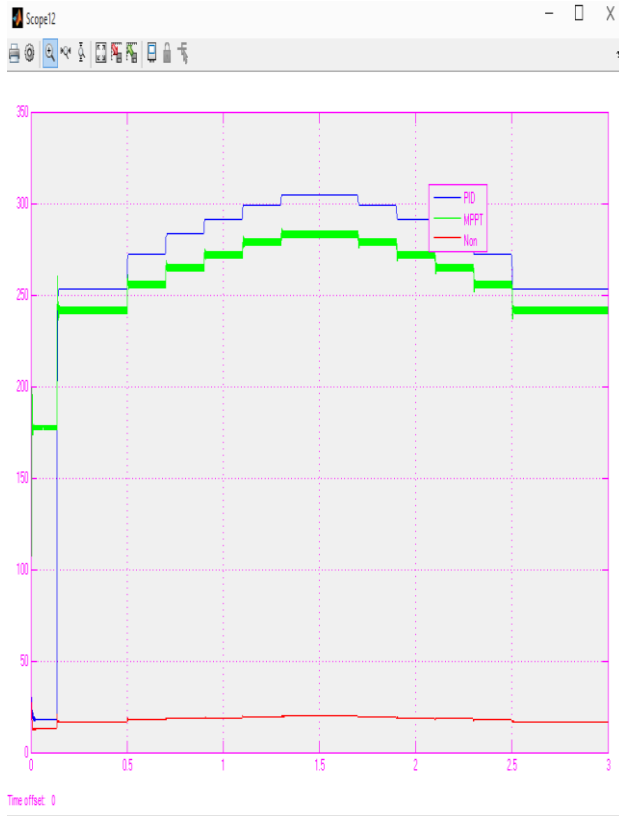


Fig. 17. RAMP Response for NO MPPT, P&O MPPT (open-loop) and PID-based MPPT (closed-loop)

The following ramp response analyses can be made for Fig 17.

11. With the ramp input, the best realized PV output power for NO MPPT is seen to be much less (about 25 W) than the attained value of 56 W for the step input.

12. As far as ramp changes in input irradiance are concerned, the PID-MPPT control mode is found to be more responsive than the P&O MPPT.

13. This is explained by the fact that the maximum output power of the PV was attained with PID control (upper curve), but the P&O (middle curve) could not attain it.

C. Impulse Response

Analyses of open-loop and closed-loop ramp responses are presented in this section. Fig. 18 shows the PV output power in response to an impulse irradiance input.

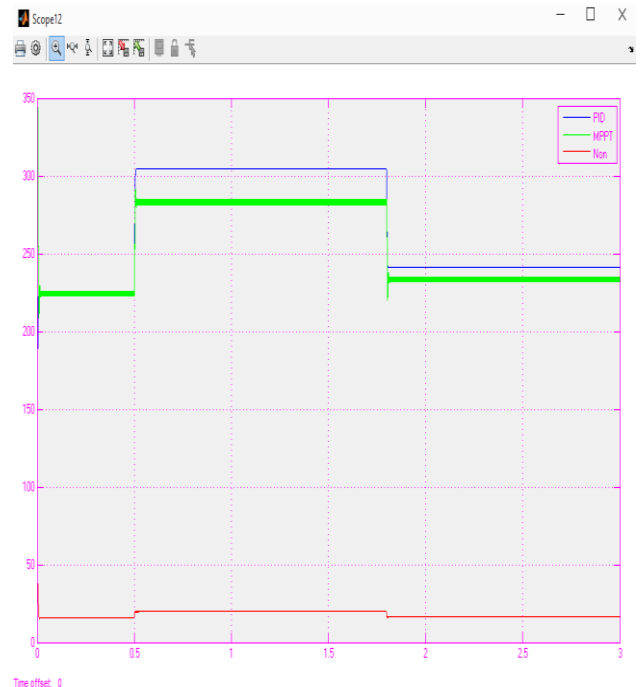


Fig. 18. IMPULSE Response for NO MPPT, P&O MPPT (open-loop) and PID-based MPPT (closed-loop)

The following impulse response analyses can be made for Fig 18.

14. With the impulse input, the best realized PV output power for NO MPPT is similar to that attained for the ramp input.

15. During a downward pulse at time 1.7 seconds, the P&O MPPT causes the output power to undershoot its mark. The system, however, quickly returns and stabilizes.

16. The PID-based MPPT controlled system however eliminates this.

17. Again, the PID-MPPT control mode is found to be more responsive than the P&O MPPT, as far as impulse changes in input irradiance are concerned.

XII. CONCLUSIONS

In this study, PID controllers and tuning methods have been reviewed. Maximum power tracking in solar PV systems have been studied.

Three systems, namely, PID-based MPPT, P&O MPPT and non-MPPT subsystems have been modeled and simulated in MATLAB/ SIMULINK to study the system's response to step, ramp and impulse signals using a commercial module, the SOLKAR 36W.

From the analysis of the results, the PID-controlled MPPT is found to be most responsive to all the various inputs. Particularly from the step response, the PID-based system had the shortest settling time of 22.7 ms (indicating the fastest system response) and zero overshoot (representing minimum losses).

The P&O MPPT performance follows that of the PID-controlled system, with a settling time of 30 ms and 224 % overshoot. The non-MPPT system gave the slowest response with settling time of 38.5 ms.

The study has proven the superiority of performance of the PID-controlled MPPT system over the P&O MPPT system for all the various signal inputs.

REFERENCES

- [1] M. A. Elgendy, B.Zahawi, and D.J. Atkinson, "Comparison of directly connected and constant voltage controlled photovoltaic pumping system", *IEEE Trans. Sustai. Energy*, vol. 1, no. 3, pp. 184-192, October 2010
- [2] J. G. Ziegler and N. B. Nichols, "Optimum settings for Automatic Controllers", *Trans. ASME*, vol. 64, 1942
- [3] G. M. van der Zalm, "Tuning of PID-Type Controllers: Literature Overview", DCT-Report nr. 2004, DAF-report nr. 51051104-50
- [4] Manoj Gogoi, "Proportional-Integral-Derivative (PID) Controller Design for Robust Stability of Arbitrary Order Plants with Time Delay and Additive Uncertainty", Bachelor of Thechnology Thesis, P.B.U.T, India, 2007
- [5] Mhamed Rebhi, Ali Benatillah, Mabrouk Sellam, Boufeldja Kadri, "Comparative Study of MPPT Controllers for PV System Implemented in the South-West of Algeria", *ScienceDirect, TerraGreen13*, International 2013-Advancements in Renewable Energy and Clean Environment, *Energy Procedia* 36 (2013), pg 142-153
- [6] Amir Gheibi, S. Mohammad Ali Mohammadi, and Malihe M. Farsangi, "Comparing performance of PID and fuzzy controllers in the presence of noise for a Photovoltaic System", *Journal of Mathematics and Computer Science (JMCS)*, Vol. 9 (2014), Issue 1, pg 69-76
- [7] S. Mallika, R. Saravanakumar, "Genetics Algorithm Based MPPT Controller for Photovoltaic System", *International Electrical Engineering Journal (IEEJ)*, Vol. 4 (2013), No. 4, pp 1159-1164, ISSN 2078-2365
- [8] J. Paulusová, M. Dúbravská, "Application of Design of PID Controller for Continuous Systems", *Institute of Control and Industrial Informatics, Slovak University of Technology, Faculty of Electrical Engineering and Information Technology*, www.google.com.gh/?gfe_rd=cr&ei=xixcVrKBbc7LoAfJ9IADA&gws_rd=ssl#q=Application+of+Design+of+PID+Controller+for+Continuous+Systems, accessed on 27.01.2016 at 12.45 GMT
- [9] Panda, Aurobinda, M.K. Pathak, S.P. Srivastava, "Fuzzy Intelligent Controller for Maximum Power Point Tracking of a Photovoltaic Module at varying atmosphere conditions", *Journal of Energy Technologies and Policy (JETP)*, Vol. 1, No. 2, 2011, ISSN: 2224-3232 (Paper), ISSN: 2225-0573 (Online), pp 18-27.
- [10] Alsayid, Basim "Modeling and Simulation of Photovoltaic Cell/Module/Array with Two-Diode Model", *International Journal of Computer Technology and Electronics Engineering (IJCTEE)* Volume 1, Issue 3, June 2012, ISSN 2249-6343
- [11] Belhaouas, N., M. S. AitCheikh, B. Amrouche, C.Larbes and A. Hadj Arab, "Matlab-Simulink libraries to Simulate PV module based on a two-diode model and their influences under shaded conditions", www.researchgate.net/...PV...twodiode_model.../9c960529b37432d2d8, accessed 07.04.14 at 23h GMT
- [12] Kurella, Amarnath, R Suresh, "Simulation of Incremental Conductance MPPT With Direct Control Method Using CUK Converter", *International Journal of Research in Engineering and Technology*, eISSN: 2319-1163; pISSN: 2321-7308
- [13] Chin, Chia Seet, BihLii Chua, Pei Yi Lim, Hui Hwang Goh and Kenneth Tze Kin Teo, "Modelling And Control of Partially Shaded Photovoltaic Arrays", *ICTACT Journal on Soft Computing*, January 2013, Volume 3, Issue 2, ISSN: 2229-6956(online)
- [14] Sera, Dezso, "Real-time Modelling, Diagnostics and Optimised MPPT for Residential PV Systems", PhD Dissertation, Faculty of Engineering, Science & Medicine, Aalborg University, pages 42-44
- [15] Huan-Liang, Tsai, Ci-Siang, Tu and Yi-Jie Su, "Development of Generalized Photovoltaic Model using MATLAB/Simulink," *Proceedings of the World Congress on Engineering and Computer Science (WCECS)*, 2008, October 22-24, San Francisco, USA, ISBN: 978-988-98671-0-2
- [16] Images: "Images for solar PV characteristics", <https://www.google.com.gh/search?q=solar+PV+cell+characteristics>, accessed 01.08.2014 at 21.30 GMT
- [17] Harjai, Arjav, Abhishek Bhardwaj, Mrutyunjaya Sandhibigraha, "Study of Maximum Power Point Tracking (MPPT) Techniques in a Solar Photovoltaic Array", Bachelor of Technology Thesis, Department of

Electrical Engineering, National Institute of Technology, Rourkela-69008, Orissa, pg 25-49

[18] Alsadi, Samer, Basim Alsayid; "Maximum Power Point Tracking Simulation for Photovoltaic Systems Using Perturb and Observe Algorithm", page 3, 4; International Journal of Engineering and Innovative Technology (IJEIT) Volume 2, Issue 6, December 2012

[19] Bratt, Jordana, "Grid connected PV Inverters: Modeling and Simulation", Master of Science Thesis, San Diego State University, 2011

[20] D. P. Holm, M. E. Ropp, "Comparative study of maximum power point tracking algorithms", Progress in Photovoltaics Research and Applications, Vol. 11, No. 1, pp 47-62, January 2003, (DOI: 10.1002/pip.459).

[21] Elgendy, Mohammed A., Bashar Zahawi, and David J. Atkinson, "Assessment of Perturb and Observe MPPT Algorithm Implementation Techniques for PV Pumping Applications", IEEE Transactions on Sustainable Energy, Vol. 3, No. 1, January 2012

[22] Wasynczuk, O., "Dynamic behaviour of a class of photovoltaic power systems", IEEE Trans. Power App. Syst., vol. PAS-102, no. 9

[23] W. T. Chee, T. C. Green, and A. H.-A. Carlos, "Analysis of perturb and observe maximum power point tracking algorithm for photovoltaic applications," presented at the 2008 IEEE 2nd Int. Power and Energy Conf. (PECon 2008), Johor Bahru, Malaysia, 2008.

[24] Femia, N., G. Petrone, G. Spagnuolo, and M. Vitelli, "A technique for improving P&O MPPT performances of double-stage grid-connected photovoltaic systems", IEEE Transactions on Industrial Electron., Vol. 56, No. 11, 2009, pp. 4473-4482, ISSN: 0278-0046, INSPEC Accession Number: 10916340, DOI: 10.1109/TIE.2009.2029589

[25] "Tuning of a PID Controller using Ziegler-Nichols Method – Lab 8", Laboratory Notes under Application of Computers in Process Control, ECET-462, Purdue University, Calumet, accessed on 20.01.2016 at 22.30 GMT at www.purduecal.edu/cpmi/NSF_Courses/_ECET-462/LABORATORIES/8-TuningofaPIDcontrollerusingZiegler-NicholsMethod.pdf

[26] Nevzat Onat, "Recent Developments in Maximum Power Point Tracking Technologies for Photovoltaic Systems", International Journal of Photoenergy, Volume 2010 (2010), Article ID 245316, pages 1-12, Hindawi Publishing Corporation, <http://dx.doi.org/10.1155/2010/245316>, Available from: https://www.researchgate.net/publication/50283080_Recent_Developments_in_Maximum_Power_Point_Tracking_Technologies_for_Photovoltaic_Systems [accessed Mar 12, 2016]